PROCEEDINGS OF SCIENCE

Determination of proton parton distribution functions using ATLAS data

Zhiqing Zhang[a,*], **on behalf of the ATLAS Collaboration**

[a] *Laboratoire de Physique des 2 infinis Irène Joliot-Curie – IJCLab, Université Paris-Saclay, Bât. 100, 15 rue Georges Clémenceau, Orsay, France*

E-mail: Zhiqing.Zhang@ijclab.in2p3.fr

We present fits to determine parton distribution functions (PDFs) using a diverse set of measurements from the ATLAS experiment at the LHC, including inclusive W and Z boson production, $t\bar{t}$ production, W+jets and Z+jets production, inclusive jet production and direct photon production. These ATLAS measurements are used in combination with deep-inelastic scattering data from HERA. Particular attention is paid to the correlation of systematic uncertainties within and between the various ATLAS data sets and to the impact of model, theoretical and parameterisation uncertainties.

41st International Conference on High Energy physics - ICHEP2022
6-13 July, 2022
Bologna, Italy

*Speaker

PoS(ICHEP2022)801

During the last decade, the ATLAS experiment [1] at the Large Hadron Collider (LHC) has used its dedicated cross section measurements [2–7] together with the deep-inelastic scattering (DIS) cross section data [8, 9] from the H1 and ZEUS experiments at HERA to constrain the parton distribution functions (PDFs) in several PDF fits [3, 10–12]. The ATLAS measurements used are inclusive W and Z boson production at 7 TeV [2] and 8 TeV [3], $t\bar{t}$ production at 8 TeV [4, 5], and W+jets and Z+jets production at 8 TeV [6, 7]. The inclusive W and Z boson production data allow the strange-quark sea distribution be determined rather than assumed to be a fixed fraction of the light-quark seas. The $t\bar{t}$ data are sensitive to the high-x gluon distribution, where x represents the fraction of the longitudinal momentum of the proton carried by the parton participating in the initial interaction. The V+jets data (with V standing generically for vector bosons W and Z) are sensitive to partons at higher x than can be accessed by inclusive W and Z boson data. The DIS data, covering a large kinematic range of negative four-momentum transfer squared, Q^2, from $O(1)$ GeV^2 to 50 000 GeV^2 and of x from 6×10^{-7} to 0.65, are the primary source of the PDF constraint. However, they do have limitations: the statistical precision of the data at high Q^2 and large x is limited and they cannot distinguish quark flavour between the down-type sea quarks, $\bar{d}$ and $\bar{s}$.

In this talk, a new PDF fit, ATLASpdf21 [13], is briefly presented. It uses, on top of the data sets mentioned above, additional $t\bar{t}$ data at 13 TeV [14], inclusive jet production at 8 TeV [15] and direct photon production 8 TeV and 13 TeV [16]. The jet production data are sensitive to the gluon distribution at medium to high x. Ratios of direct photon production at different proton–proton collision energies have only a mild impact on the gluon distribution, but they may now be reliably fitted to next-to-next-leading (NNLO) order in perturbative quantum chromodynamics (QCD), as all other data sets considered in the fit.

The ATLASpdf21 fit uses the xFitter framework [8, 17]. It interfaces to theoretical calculations directly or uses fast interpolation grids to make theoretical predictions in NNLO in QCD and next-to-leading order for electroweak effects for the considered processes. It differs from the previous ATLAS PDF fits mainly in that it uses a diverse set of measurements from the ATLAS experiments and the fit is made without any constraints imposed on the relation between $x\bar{u}$, $x\bar{d}$ and $x\bar{s}$. The PDFs are parameterised in x for a starting scale Q_0^2 at 1.9 GeV^2 so that it is below the charm mass threshold. The PDFs at other scale are obtained using the DGLAP evolution equations [18–20]. The free parameters of the PDFs are determined by minimising χ^2 between the data and the predictions.

The impact of each data set is studied. One example is shown in Figure 1a comparing at Q_0^2 the ratio of strange-quark seas over up- and down-quark seas from the nominal fit determined with a tolerance value of $T^2 = \Delta\chi^2 = 1$ with that from a fit where the inclusive W and Z boson production data are removed. It shows that the ratio cannot be determined reliably without the inclusive weak boson data.

The correlations of systematic uncertainties between different data sets are also studied. When the correlations between the V+jets, $t\bar{t}$ and inclusive jet data sets are not applied, the central values and uncertainty bands of the PDFs are found to be different from the nominal one. The change for the strange-quark sea is presented in Figure 1b at $Q^2 = 10\,000$ GeV^2, a scale relevant for precision LHC physics, showing the importance to take into account the inter-data-set correlations.

When including the data at high energy scales in the fit, the possibility of subtle effects of beyond standard model (BSM) physics may be absorbed in the PDFs. To check this, a fit is performed in which the maximum scale for measurements accepted from each process is 500 GeV,

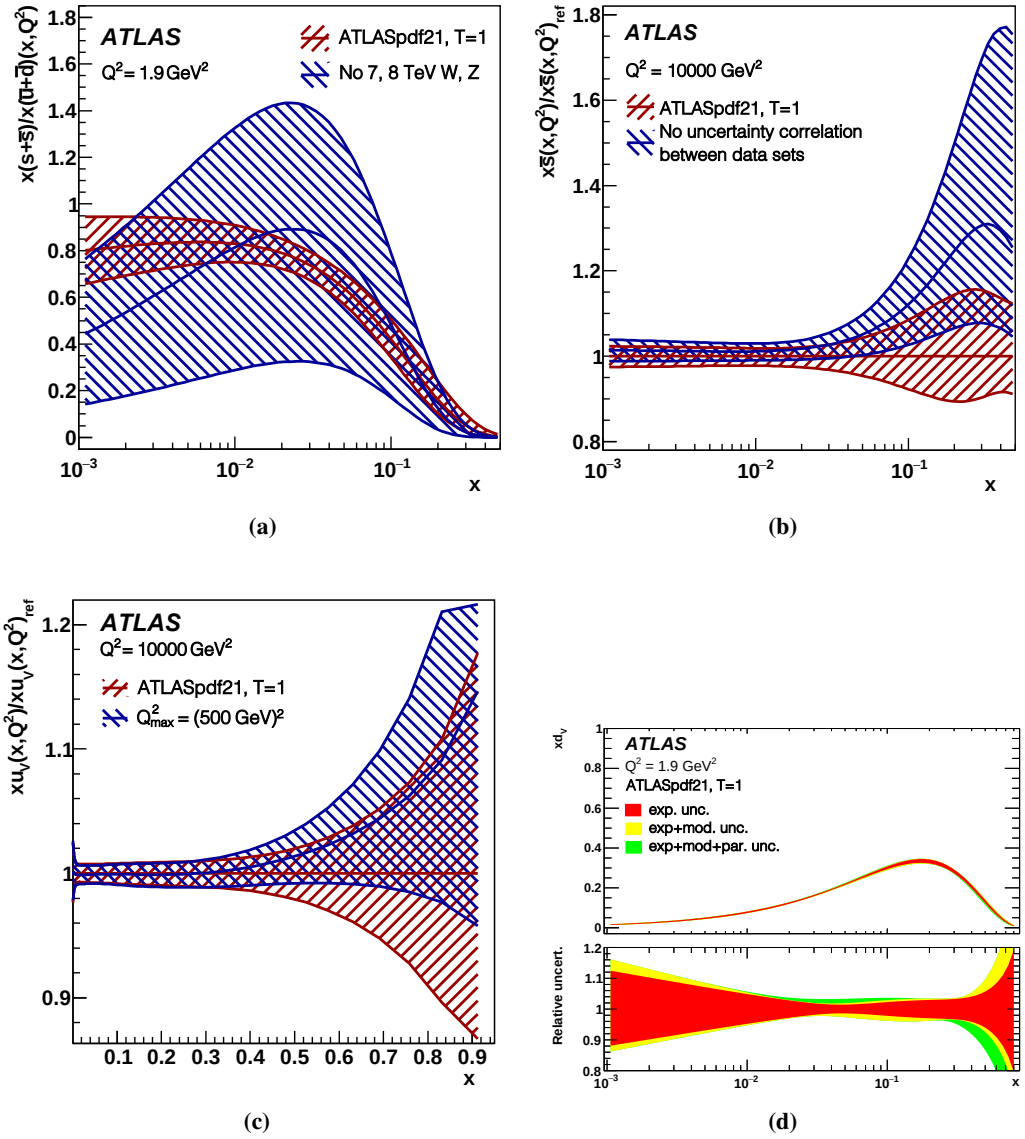

Figure 1: (a) Ratio of $R_s = x(s+\bar{s})/x(\bar{u}+\bar{d})$ from the ATLASpdf21 fit compared with R_s from a fit not including the inclusive vector boson data. (b) Ratio of the strange quark sea distribution extracted from the ATLASpdf21 fit including correlations of systematic uncertainties between data sets to that extracted from a fit in which only the luminosity uncertainties for each centre-of-mass energy are correlated between data sets. (c) Ratio of the up valence quark distribution shown in linear x scale from a fit in which a maximum scale of 500 GeV is imposed, to the ATLASpdf21 fit. (d) Distribution of the down valence quark comparing experimental uncertainties (red), model (yellow) and parameterisation (green) uncertainties. In (a)-(c), the error bands correspond to experimental uncertainties (including a small contribution of theoretical scale uncertainties). The experimental uncertainties are evaluated with tolerance $T = 1$ in all plots. Plots (a) and (d) are shown at $Q_0^2 = 1.9\,\text{GeV}^2$, while (b) and (c) at $Q^2 = 10\,000\,\text{GeV}^2$. Plots are from Ref. [13].

$Q^2 = 250\,000\,\text{GeV}^2$. Figure 1c compares the up valence quark distribution at the scale of $Q^2 = 10\,000\,\text{GeV}^2$, with a linear scale in x to emphasise the difference at high x. Given the current precision on the PDFs, the BSM effect is not yet significant.

So far, the uncertainty bands shown in Figure 1a-1c correspond only to the experimental uncertainties of the fit. Additional model, theoretical and parameterisation uncertainties are also considered. The model uncertainties include effects due to variations of heavy-quark mass input to the heavy-flavour scheme used for the inclusive DIS calculations, the minimum Q^2 cut on the HERA inclusive DIS data and the value of the starting scale for evolution. Further model uncertainties come from the assumed value of the top-quark mass, the treatment of the jet systematic uncertainties, and the choice of jet radius for the inclusive jet data. Theoretical uncertainties include the scale uncertainties of the predictions, the largest being for the inclusive W and Z boson data. The parameterisation uncertainties correspond to the effect on the PDFs by adding extra parameters to the optimal number of parameters of the nominal PDFs determined by the saturation method of the χ^2 fit [13]. In general, the experimental uncertainties are by far the dominant uncertainty source. The size of the other uncertainties is only visible for some of the PDFs, e.g. for the down valence quark distribution shown in Figure 1d. For technical reasons the small theoretical uncertainty is included in the experimental uncertainty evaluation.

The nominal ATLASpdf21 fit has a total χ^2 value of 2010 for 1620 degrees of freedom indicating the choice of $T = 1$ is not optimal for defining the size of the experimental uncertainties of the PDFs. A study to find an appropriate tolerance using the dynamic tolerance procedure introduced in the MSTW paper [21] was performed. The tolerance $T = 3$ is applied to the

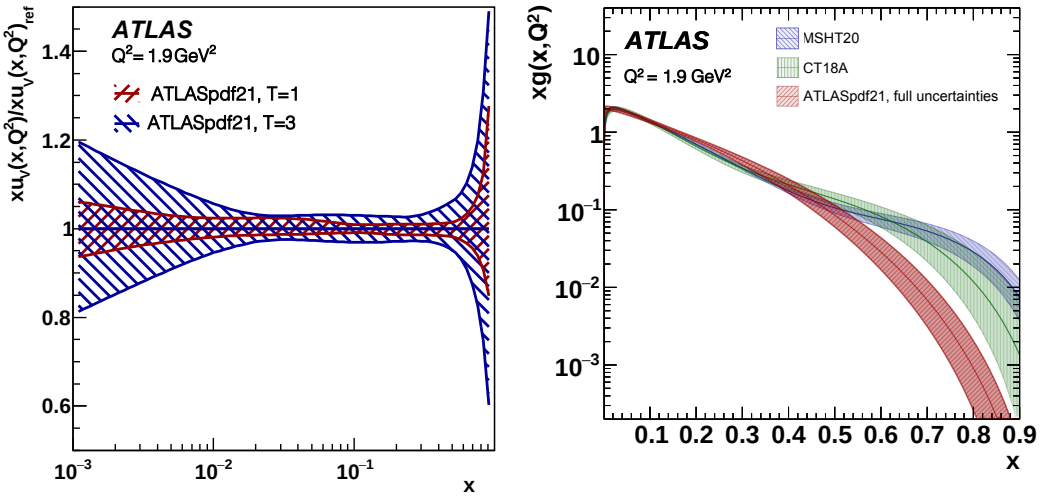

Figure 2: (a) Comparison of the full uncertainties (experimental, model and parameterisation) of the up valence quark distribution of the ATLASpdf21 fit for tolerance value $T = 1$ and $T = 3$; (b) Comparison of the gluon distribution of the ATLASpdf21 fit with full uncertainties (experimental $T = 3$, model and parameterisation) with MSHT20 and CT18A global PDFs, showing in linear x scale to focus on high x behaviour. Plots are from Ref. [13].

experimental uncertainties for the final estimation of PDF uncertainty. With this choice, the model and parameterisation uncertainties are far less significant. The full uncertainties are compared for the choices $T = 3$ and $T = 1$ in Figure 2a for the up valence quark distribution.

The ATLASpdf21 PDFs are compared with other global PDFs. An example for the gluon distribution between ATLASpdf21 and CT18A [22] and MSHT20 [23] PDFs is compared in Figure 2b in linear x scale to focus more on the high x regime, which is important in searches for new physics. Some discrepancies appear at very high x where there is no data to determine any of the PDFs.

To conclude, ATLAS has performed a new PDF fit, ATLASpdf21 [13], using diverse ATLAS data sets in combination with deep-inelastic scattering data from HERA. It is observed that the addition of the ATLAS data sets to the HERA data brings the PDFs much closer to those of the global fits than to HERAPDF2.0 [9, 13]. The ATLAS data seem able to replicate most of the features that the fixed-target DIS and Drell-Yan data plus the Tevatron data brought to the global PDFs. Using only the HERA and ATLAS data allows a more rigorous treatment of correlated systematic uncertainties and especially of correlations between data sets. More precise measurements in extended kinematic regions and improved theoretical predictions are needed to further improve our knowledge on the PDFs.

References

[1] ATLAS Collaboration, JINST **3** (2008), S08003 doi:10.1088/1748-0221/3/08/S08003.

[2] ATLAS Collaboration, Phys. Rev. D **85** (2012) 072004 doi:10.1103/PhysRevD.85.072004 [arXiv:1109.5141 [hep-ex]].

[3] ATLAS Collaboration, Eur. Phys. J. C **77** (2017) 367 doi:10.1140/epjc/s10052-017-4911-9 [arXiv:1612.03016 [hep-ex]].

[4] ATLAS Collaboration, Eur. Phys. J. C **76** (2016) 538 doi:10.1140/epjc/s10052-016-4366-4 [arXiv:1511.04716 [hep-ex]].

[5] ATLAS Collaboration, Phys. Rev. D **94** (2016) 092003 doi:10.1103/PhysRevD.94.092003 [arXiv:1607.07281 [hep-ex]].

[6] ATLAS Collaboration, JHEP **05** (2018) 077 [erratum: JHEP **10** (2020) 048] doi:10.1007/JHEP05(2018)077 [arXiv:1711.03296 [hep-ex]].

[7] ATLAS Collaboration, Eur. Phys. J. C **79** (2019) 847 doi:10.1140/epjc/s10052-019-7321-3 [arXiv:1907.06728 [hep-ex]].

[8] H1 and ZEUS Collaborations, JHEP **01** (2010) 109 doi:10.1007/JHEP01(2010)109 [arXiv:0911.0884 [hep-ex]].

[9] H1 and ZEUS Collaborations, Eur. Phys. J. C **75** (2015) 580 doi:10.1140/epjc/s10052-015-3710-4 [arXiv:1506.06042 [hep-ex]].

[10] ATLAS Collaboration, Phys. Rev. Lett. **109** (2012) 012001 doi:10.1103/PhysRevLett.109.012001 [arXiv:1203.4051 [hep-ex]].

[11] ATLAS Collaboration, ATL-PHYS-PUB-2018-017, URL: https://cds.cern.ch/record/2633819.

[12] ATLAS Collaboration, JHEP **07** (2021) 223 doi:10.1007/JHEP07(2021)223 [arXiv:2101.05095 [hep-ex]].

[13] ATLAS Collaboration, Eur. Phys. J. C **82** (2022) 438 doi:10.1140/epjc/s10052-022-10217-z [arXiv:2112.11266 [hep-ex]].

[14] ATLAS Collaboration, Eur. Phys. J. C **79** (2019) 1028 [erratum: Eur. Phys. J. C **80** (2020) no.11, 1092] doi:10.1140/epjc/s10052-019-7525-6 [arXiv:1908.07305 [hep-ex]].

[15] ATLAS Collaboration, JHEP **05** (2018) 195 doi:10.1007/JHEP05(2018)195 [arXiv:1711.02692 [hep-ex]].

[16] ATLAS Collaboration, JHEP **04** (2019) 093 doi:10.1007/JHEP04(2019)093 [arXiv:1901.10075 [hep-ex]].

[17] S. Alekhin, O. Behnke, P. Belov, S. Borroni, M. Botje, *et al.* Eur. Phys. J. C **75** (2015) no.7, 304 doi:10.1140/epjc/s10052-015-3480-z [arXiv:1410.4412 [hep-ph]].

[18] V. N. Gribov and L. N. Lipatov, Sov. J. Nucl. Phys. **15** (1972) 438 IPTI-381-71.

[19] G. Altarelli and G. Parisi, Nucl. Phys. B **126** (1977) 298 doi:10.1016/0550-3213(77)90384-4.

[20] Y. L. Dokshitzer, Sov. Phys. JETP **46** (1977) 641.

[21] A. D. Martin, W. J. Stirling, R. S. Thorne and G. Watt, Eur. Phys. J. C **63** (2009) 189 doi:10.1140/epjc/s10052-009-1072-5 [arXiv:0901.0002 [hep-ph]].

[22] T. J. Hou, J. Gao, T. J. Hobbs, K. Xie, S. Dulat, *et al.* Phys. Rev. D **103** (2021) 014013 doi:10.1103/PhysRevD.103.014013 [arXiv:1912.10053 [hep-ph]].

[23] S. Bailey, T. Cridge, L. A. Harland-Lang, A. D. Martin and R. S. Thorne, Eur. Phys. J. C **81** (2021) 341 doi:10.1140/epjc/s10052-021-09057-0 [arXiv:2012.04684 [hep-ph]].

PoS(ICHEP2022)801